Electronic Supplementary Material (ESI) for Journal of Materials Chemistry C.

Electronic Supplementary Information

Asymmetric-Triazine-Cored Triads as Thermally Activated Delayed Fluorescence Emitters for High-Efficiency Yellow OLEDs with Slow Efficiency Roll-Off

Yepeng Xiang,[a,†] *Shaolong Gong,*[a,†] *Yongbiao Zhao,*[b] *Xiaojun Yin,*[a] *Jiajia Luo,*[a]
Kailong Wu,[a] *Zheng-Hong Lu,**[b] *Chuluo Yang**[a]

Y. Xiang, Dr. X. Yin, J. Luo, K. Wu, Prof. S. Gong and Prof. C. Yang
Hubei Collaborative Innovation Center for Advanced Organic Chemical Materials, Hubei Key Lab on Organic and Polymeric Optoelectronic Materials, Department of Chemistry, Wuhan University, Wuhan 430072, People's Republic of China
*E-mail: clyang@whu.edu.cn

Dr. Y. Zhao and Prof. Z.-H. Lu
Department of Materials Science and Engineering, University of Toronto, 184 College St., Toronto, Ontario M5S 3E4, Canada
*E-mail: zhenghong.lu@utoronto.ca

General information

All the reagents and solvents used for the synthesis or measurements were commercially available, and used as received unless otherwise stated. The ^{1}H NMR and ^{13}C NMR spectra were recorded on a MERCURY-VX300 spectrometer with $CDCl_3$ as the solvent and tetramethylsilane (TMS) as an internal reference. Elemental analysis of carbon, hydrogen, and nitrogen was performed on a Vario EL III microanalyzer. Molecular masses were determined by Fourier Transform Ion Cyclotron Resonance Mass Spectrometer. Thermogravimetric analysis (TGA) and differential scanning calorimetry (DSC) were performed on NETZSCH STA 449C instrument and NETZSCH DSC 200 PC unit under a nitrogen atmosphere, respectively. The thermal stability of the samples was determined by measuring their weight loss, heated at a rate of 10°C min^{-1} from room temperature to 600°C. The glass transition temperature (T_g) was determined from the second heating scan at a heating rate of 10°C min^{-1} from -60 to 320°C. UV−Vis absorption spectra were recorded on a Shimadzu UV-2501 recording spectrophotometer with baseline correction. Photoluminescence (PL) spectra were recorded on a Hitachi F-4600 fluorescence spectrophotometer. Cyclic voltammetric (CV) studies of the compounds were carried out in nitrogen-purged dichloromethane (CH_2Cl_2) at room temperature with a CHI voltammetric analyzer. n-Bu_4PF_6 (0.1 M) was used as the supporting electrolyte. The conventional three-electrode configuration consists of a platinum working electrode, a platinum wire auxiliary electrode, and an Ag wire pseudo-reference electrode with ferrocene (Fc/Fc$^+$) as the internal standard. The HOMO energy levels (eV) of the compounds were calculated according to the formula: $-[4.8+(E_{1/2(ox/red)}-E_{1/2(Fc/Fc^+)})]$eV. The LUMO energy levels (eV) of the compounds were calculated according to the formula: $-[4.8-(E_{1/2(red/ox)}-E_{1/2(Fc/Fc^+)})]$eV. The PL lifetimes was measured by a single photon counting spectrometer from Edinburgh Instruments (FLS920) with a Picosecond Pulsed UV-LASTER (LASTER377) as the excitation source. Absolute PLQYs were obtained using a Quantaurus-QY measurement system (C9920-02, Hamamatsu Photonics) and all the samples were excited at 380 nm.

Device fabrication and measurement.

The electron-injection material of LiF was purchased from Sigma-Aldrich and used as received. The hole-transporting materials of tris(4-(9*H*-carbazol-9-yl)phenyl)amine (TCTA) and 4,4'-(cyclohexane-1,1-diyl)bis(*N,N*-di-p-tolylaniline) (TAPC), host material of 4,4'-di(9*H*-carbazol-9-

yl)-1,1'-biphenyl (CBP), and electron transport material of 1,3,5-tri(*m*-pyrid-3-yl-phenyl)benzene (TmPyPB) were purchased from Luminescence Technology Corporation and used as received. Devices were fabricated in a Kurt J. Lesker LUMINOS cluster tool with a base pressure of 10^{-7}Torr without breaking vacuum. The ITO anode was commercially patterned and coated on glass substrates with a thickness of 120 nm and sheet resistance of 15 Ω per square. Prior to loading, the substrate was degreased with standard solvents, blow-dried using a N_2 gun, and treated in a UV−ozone chamber. The active area for all devices was 2 mm^2. Before removing the devices from the vacuum for characterization they were encapsulated by a 500 nm thick layer of SiO_2 deposited by thermal evaporation. Luminance−voltage measurements were carried out using a Minolta LS-110 Luminance Meter. Current−voltage characteristics were measured using an HP4140B pA meter. The electroluminescence spectra were measured using an Ocean Optics USB4000 spectrometer calibrated with a standard halogen lamp. The radiant flux for calculating EQEs was measured using an integrating sphere equipped with an Ocean Optics USB4000 spectrometer with NIST traceable calibration using a halogen lamp.

Synthesis of materials

All reagents were used as received from commercial sources and used as received unless otherwise stated.

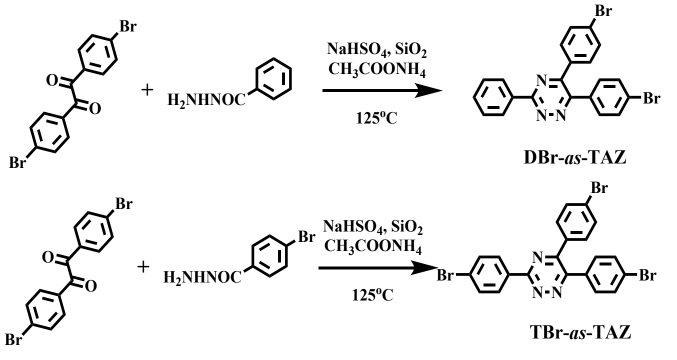

Scheme S1. Synthesis of DBr-*as*-TAZ and TBr-*as*-TAZ.

5,6-Bis(4-bromophenyl)-3-phenyl-1,2,4-triazine (DBr-*as*-TAZ): A mixture of benzohydrazide (136 mg, 1 mmol), 1,2-bis(4-bromophenyl)ethane-1,2-dione (368 mg, 1 mmol), ammonium acetate (231 mg, 3 mmol) and $NaHSO_4/SiO_2$ (200 mg) was thoroughly mixed in a mortar and then heated in the oil bath at 125 °C for 6 h. The mixture was cooled down to room temperature and mixed thoroughly with 3 × 20 mL of dichloromethane. The collected organic phase was washed with water and dried with anhydrous Na_2SO_4. After filteration and removal of the solvent, the residue was purified by column chromatography on silica gel (eluent: petroleum /dichloromethane = 1:1, v/v) to afford the title compound as white powder (242 mg, yield: 52%). ^{1}H NMR (300 MHz, $CDCl_3$ + TMS, 25 ^{o}C) δ [ppm]: 8.66-8.63 (m, 2H), 7.59-7.49 (m, 11H). ^{13}C NMR (75 MHz, $CDCl_3$, 25 ^{o}C) δ [ppm]: δ 161.62, 154.52, 134.65, 134.33, 132.33, 132.27, 132.13, 131.57, 131.16, 129.17, 128.63, 126.12, 124.77. MS (EI): *m/z* 466.91 [M$^+$]. Anal. Calcd for $C_{21}H_{13}N_3Br_4$: C 53.99, H 2.81, N 8.99. found: C 53.90, H 2.75, N 9.01

3,5,6-Tris(4-bromophenyl)-1,2,4-triazine (TBr-*as*-TAZ): The title compound was synthesized according to the similar procedure as DBr-i-TAZ, but with 4-bromobenzohydrazide (215 mg, 1 mmol) to replace benzohydrazid. Yield: 32%. ^{1}H NMR (300 MHz, $CDCl_3$ + TMS, 25 ^{o}C) δ [ppm]: 8.51 (d, J = 8.7 Hz, 2H), 7.70 (d, J = 9.0 Hz, 2H), 7.58-7.48 (m, 8H). ^{13}C NMR (75 MHz, $CDCl_3$, 25 ^{o}C) δ [ppm]: 160.60, 154.40, 154.28, 134.14, 133.88, 133.22, 132.11, 132.04, 132.00, 131.21, 130.81, 129.75, 126.78, 125.94, 124.59. MS (EI): *m/z* 546.13 [M$^+$]. Anal. Calcd for $C_{21}H_{12}N_3Br_3$: C 46.19, H 2.22, N 7.70. found: C 46.10, H 2.32, N 7.59.

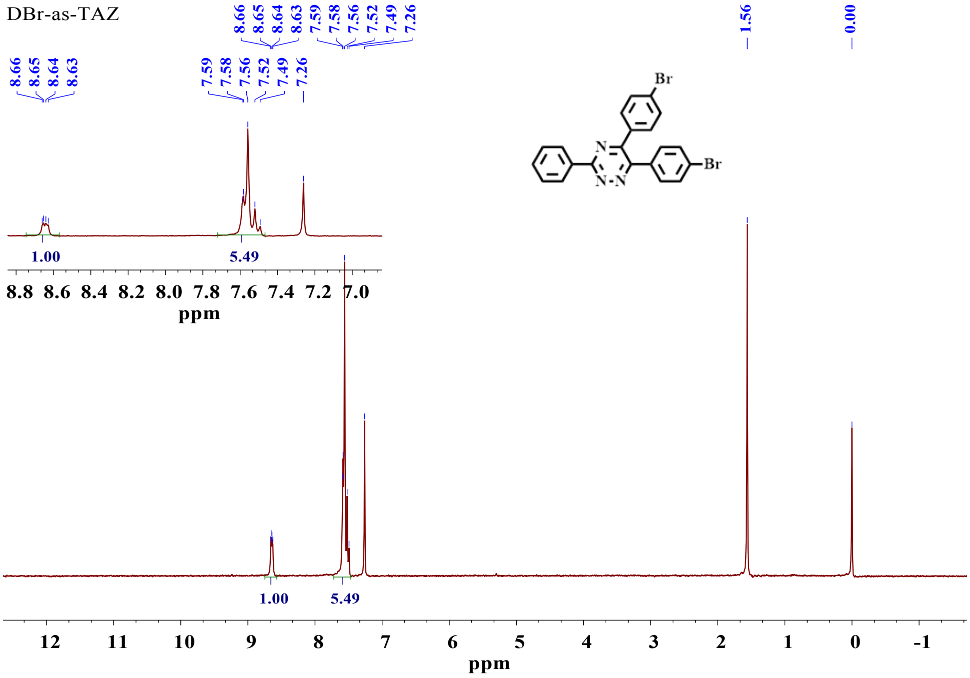

Fig. S1 ^{1}H NMR spectra of DBr-*as*-TAZ (300 MHz, $CDCl_3$ + TMS, 25 °C).

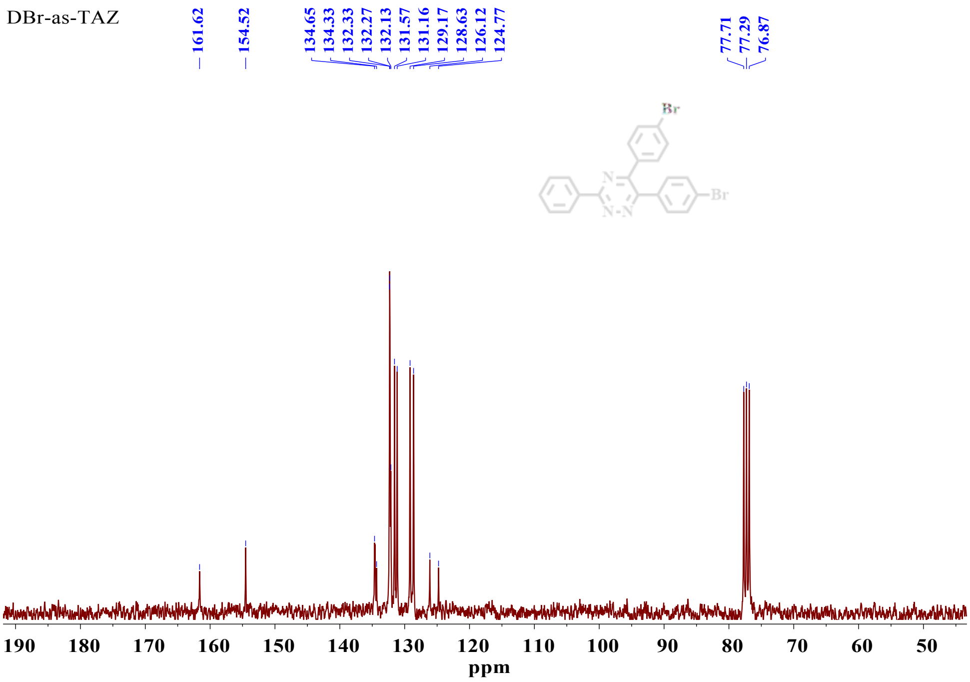

Fig. S2 ^{13}C NMR spectra of DBr-*as*-TAZ (75 MHz, $CDCl_3$, 25 °C).

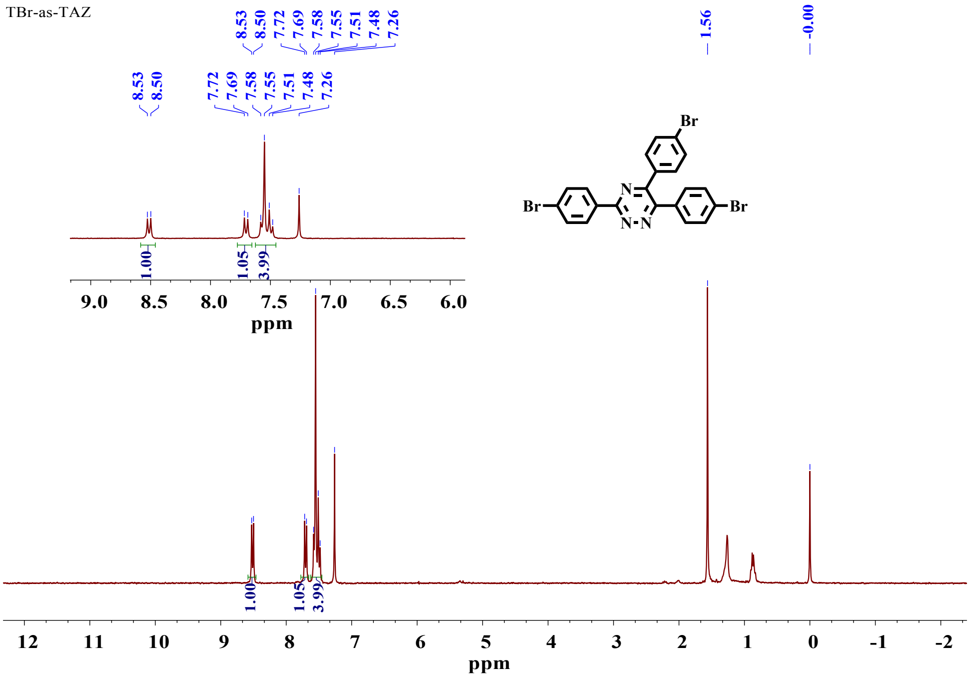

Fig. S3 ^{1}H NMR spectra of TBr-*as*-TAZ (300 MHz, $CDCl_3$ + TMS, 25 °C).

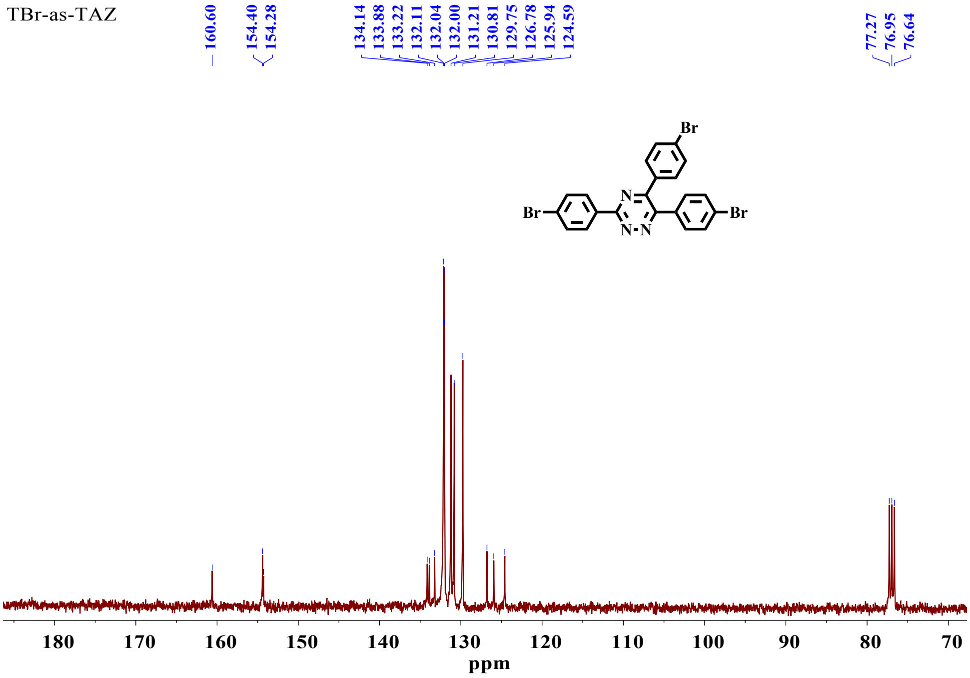

Fig. S4 ^{13}C NMR spectra of TBr-*as*-TAZ (75 MHz, CDCl$_3$, 25 ^{o}C).

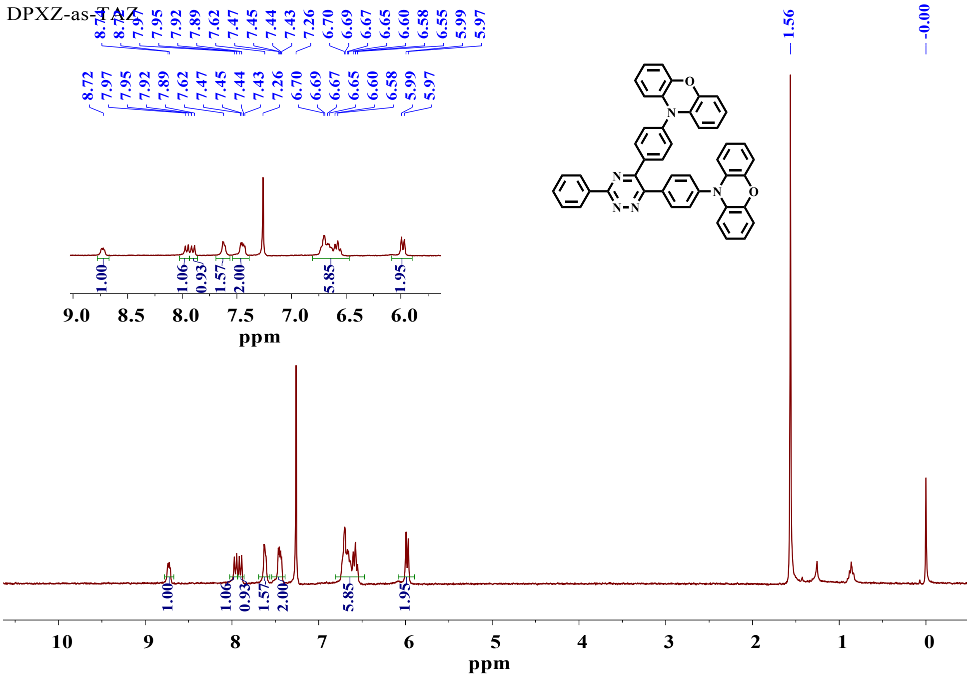

Fig. S5 ^{1}H NMR spectra of DPXZ-*as*-TAZ (300 MHz, CDCl$_3$ + TMS, 25 ^{o}C).

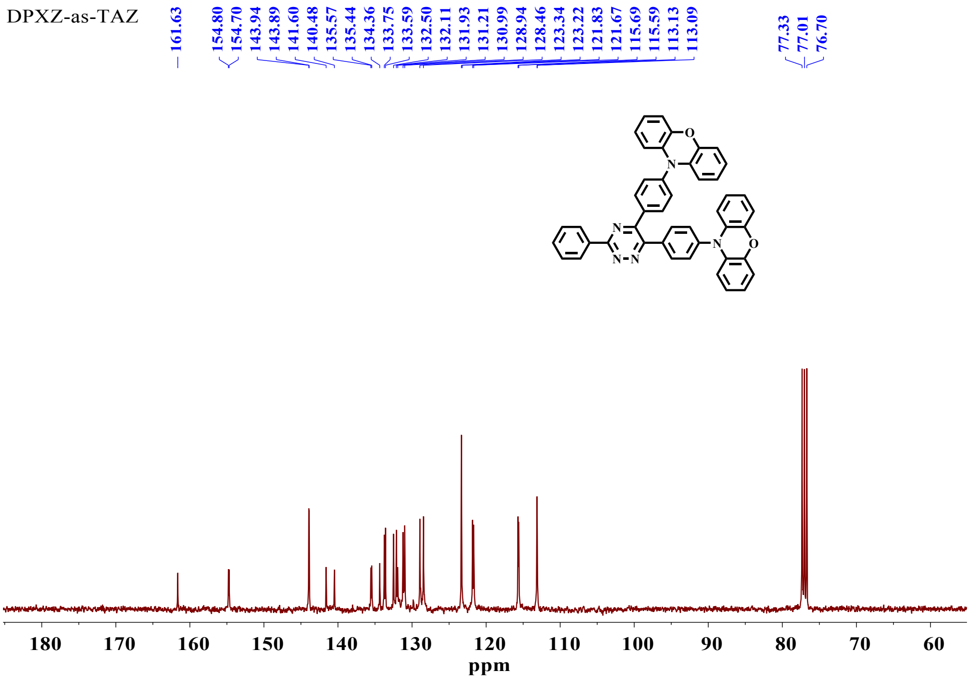

Fig. S6 ^{13}C NMR spectra of DPXZ-*as*-TAZ (75 MHz, $CDCl_3$, 25 °C).

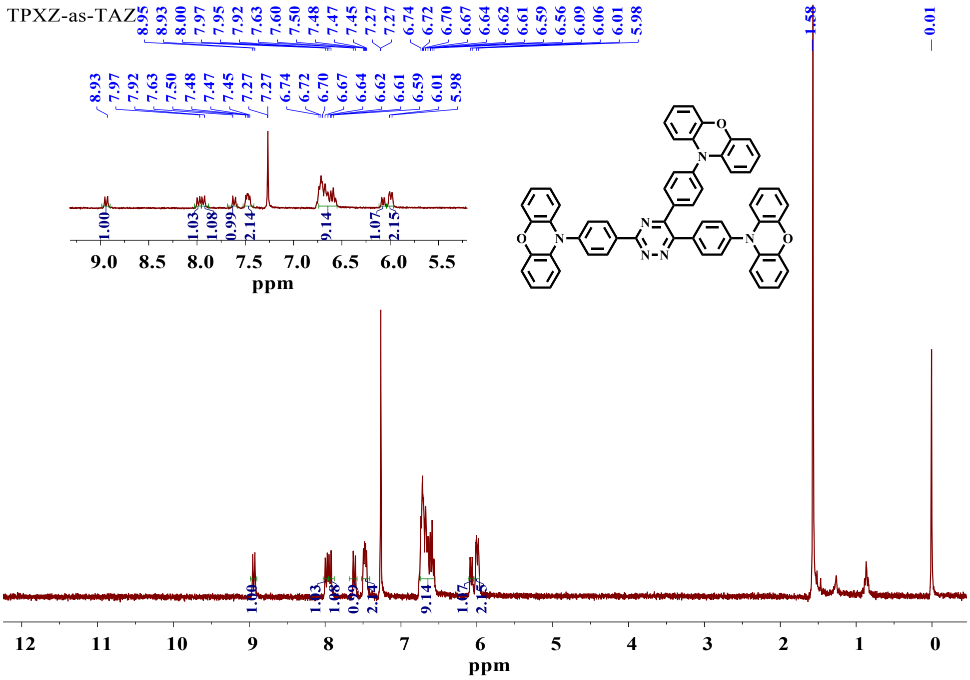

Fig. S7 ^{1}H NMR spectra of TPXZ-*as*-TAZ (300 MHz, $CDCl_3$ + TMS, 25 °C).

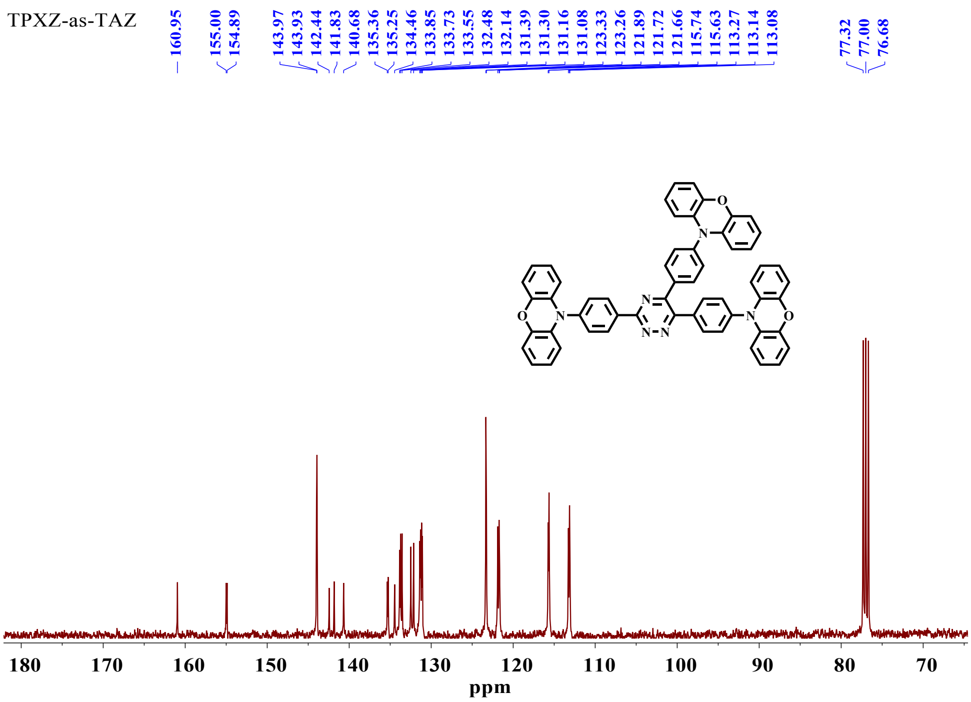

Fig. S8 ^{13}C NMR spectra of TPXZ-*as*-TAZ (75 MHz, CDCl$_3$, 25 ^{o}C).

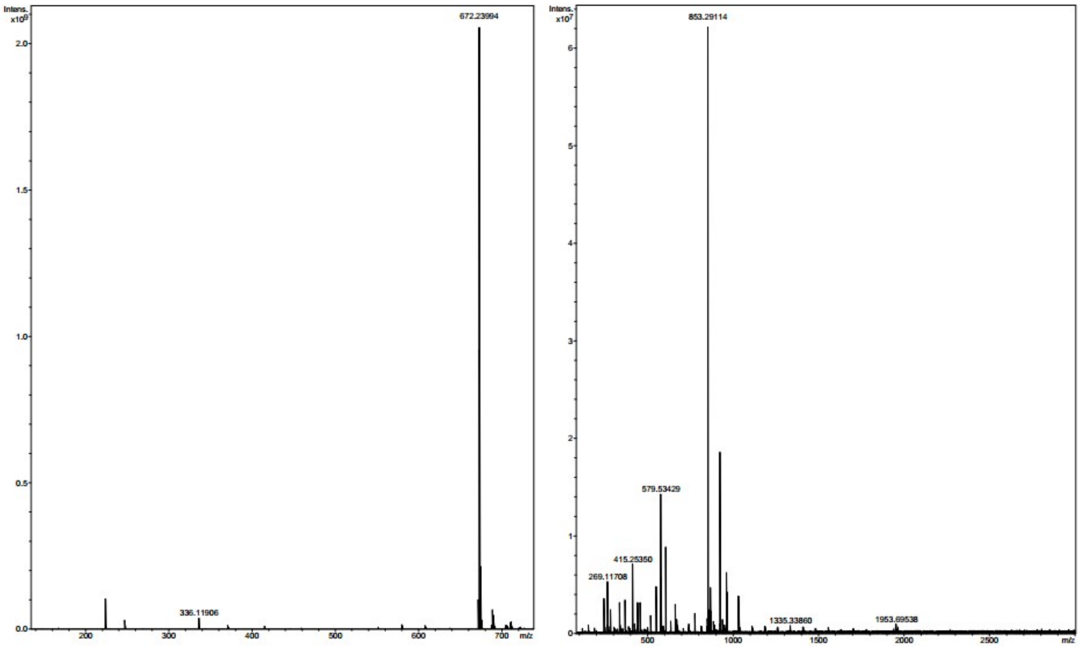

Fig. S9 High-resolution Mass data of DPXZ-*as*-TAZ and TPXZ-*as*-TAZ.

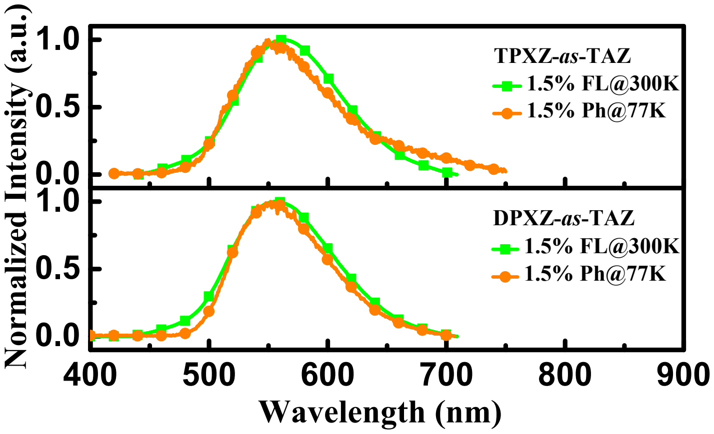

Fig. S10 The fluorescence and phosphorescence spectra of the DPXZ-*as*-TAZ and TPXZ-*as*-TAZ in 1.5 wt% PMMA doped films.

Table S1. Photophysical data of the two compounds in PMMA doped films

Compounds	$S_1{}^a$ [eV]	$T_1{}^b$ [eV]	$\Delta E_{ST}{}^c$ [eV]
DPXZ-*as*-TAZ	2.59	2.52	0.07
TPXZ-*as*-TAZ	2.55	2.53	0.02

[a]Calculated from the onset of the fluorescence spectra of two emitters doped into PMMA (1.5 wt%) at room temperature. [b]Calculated from the onset of the phosphorescence spectra of two emitters doped into PMMA (1.5 wt%) at room temperature. [c]$\Delta E_{ST} = S_1{}^a - T_1{}^b$.

Table S2 Electroluminescence characteristics of the devices

Device	Emitter	Doping concentration (wt%)	EQE_{max} (%)
A_1	DPXZ-*as*-TAZ	1.5	9.6
A_2	DPXZ-*as*-TAZ	3	9.1
A_3	DPXZ-*as*-TAZ	6	9.4
A_4	DPXZ-*as*-TAZ	9	9.1

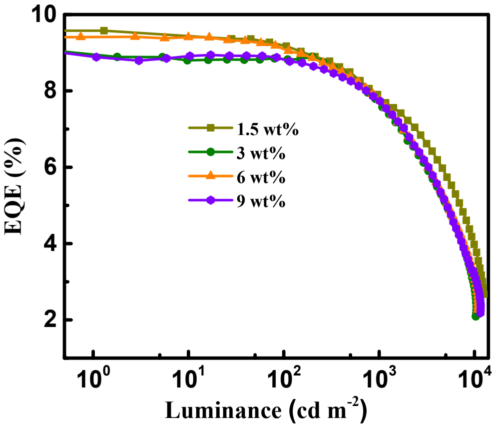

Fig. S11 The maximum external quantum efficiency (EQE$_{max}$) *versus* luminance curves by changing doping concentration for devices with the structure of ITO/TAPC (30 nm)/TCTA (5 nm)/CBP: x wt% DPXZ-*as*-TAZ (15 nm)/Tm3PyPB (65 nm)/LiF (0.8 nm)/Al (80 nm), where x = 1.5, 3, 6, and 9.

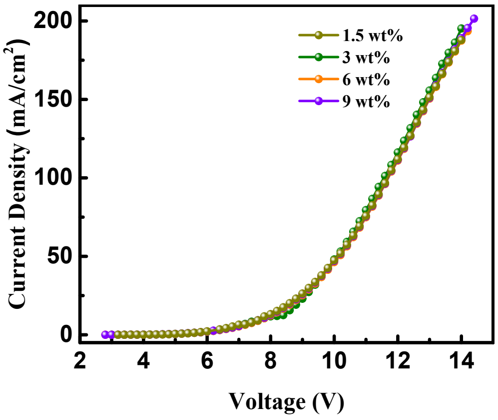

Fig. S12 Current density *versus* voltage characteristics as a function of doping concentration for devices with the structure of ITO/TAPC (30 nm)/TCTA (5 nm)/CBP: x wt% DPXZ-*as*-TAZ (15 nm)/Tm3PyPB (65 nm)/LiF (0.8 nm)/Al (80 nm), where x = 1.5, 3, 6, and 9.

Table S3. Comparison of EL data of the devices employed yellow/orange TADF materials as emitters at a luminance of 1000 cd/m^2.

Compounds	EQE^a (%)	EQE Roll-Off^b (%)	Ref.
TPXZ-*as*-TAZ	11.5	11.5	This work
TXO-TPA	~6	~67.6	1
PPZ-DPO	~5	~50.0	2
ACRDSO2	13.1	31.8	3
Ac-CNP	9.1	31.6	4

[a]The external quantum efficiency at 1000 cd/m^2. [b]The external quantum efficiency at 1000 cd/m^2 *versus* the maximum external quantum efficiency.

Table S4. Comparison of EL data of the devices employed blue/green TADF materials based on triazine core as emitters at a luminance of 1000 cd/m^2.

Compounds	EQE[a] (%)	EQE Roll-Off[b] (%)	Emission	Ref.
DACT-II	~21.0	~29.1	green	5
1a	~2.5	~72.2	green	6
2a	11.0	50.9	sky-blue	6
2b	6.0	67.6	sky-blue	6
2c	4.6	70.5	sky-blue	6
PXZ-TRZ	~10	~20	green	7
DCzTrz	13.0	27.0	blue	8
DDCzTrz	3	84.1	sky-blue	8
TCzTrz	~12	~52.0	sky-blue	9
TmCzTrz	~13.5	~47.1	green	9
DCzmCZTrz	~12	~43.7	green	9
DMAC-TRZ	22.5	15.1	green	10
DPAC-TRZ	18.3	29.1	sky-blue	11
SpiroAC-TRZ	30.5	16.9	sky-blue	11

[a]The external quantum efficiency at 1000 cd/m^2. [b]The external quantum efficiency at 1000 cd/m^2 *versus* the maximum external quantum efficiency.

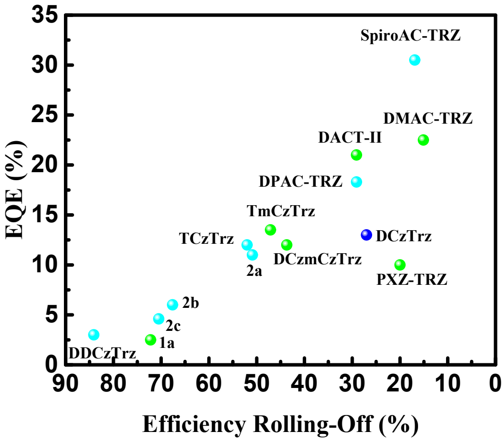

Fig. S13 EQE *versus* EQE roll-off of high-efficiency based on triazine core blue/green TADF materials as emitters OLEDs at a luminance of 1000 cd/m^2 from literature. Device data are taken from Ref.[5-11]. The color of points are represented their emissions in EL process.

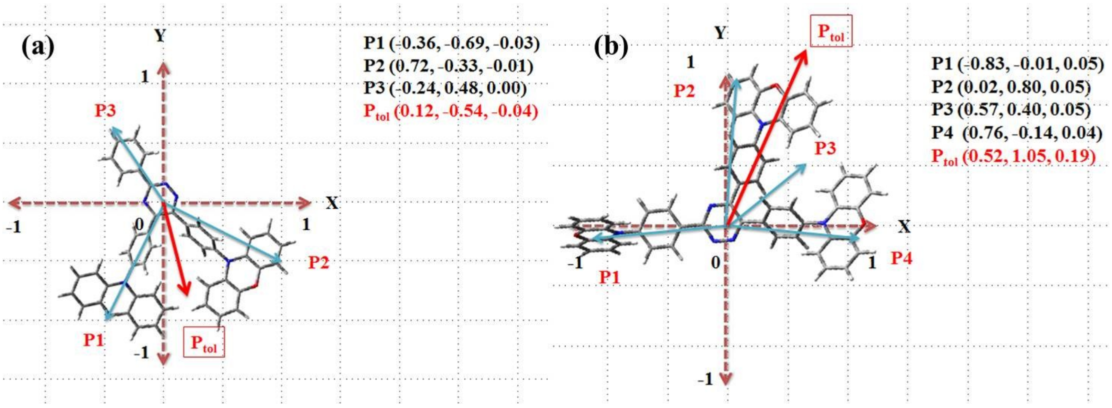

Fig. S14 The total orientations of the transition dipole moments in (a) DPXZ-*as*-TAZ and (b) TPXZ-*as*-TAZ. Optimized molecular structure and transition dipole moments calculated by TD-DFT B3LYP/6-31+G(d,p) for the lowest transition from the ground (S_0) to the excited state (S_1) originating from possible transitions with almost equivalent transition probabilities.

References:

1. H. Wang, L. Xie, Q. Peng, L. Meng, Y. Wang, Y. Yi and P. Wang, *Adv. Mater.*, 2014, **26**, 5198-5204.
2. Q. Zhang, B. Li, S. Huang, H. Nomura, H. Tanaka and C. Adachi, *Nat. Photon.*, 2014, **8**, 326-332.
3. G. Xie, X. Li, D. Chen, Z. Wang, X. Cai, D. Chen, Y. Li, K. Liu, Y. Cao and S.-J. Su, *Adv. Mater.*, 2016, **28**, 181-187.
4. I. S. Park, S. Y. Lee, C. Adachi and T. Yasuda, *Adv. Funct. Mater.*, 2016, **28**, 4626-4633.
5. H. Kaji, H. Suzuki, T. Fukushima, K. Shizu, K. Suzuki, S. Kubo, T. Komino, H. Oiwa, F. Suzuki, A. Wakamiya, Y. Murata and C. Adachi, *Nat. Commun.*, 2015, **6**.
6. S. Hirata, Y. Sakai, K. Masui, H. Tanaka, S. Y. Lee, H. Nomura, N. Nakamura, M. Yasumatsu, H. Nakanotani, Q. Zhang, K. Shizu, H. Miyazaki and C. Adachi, *Nat. Mater.*, 2015, **14**, 330-336.
7. H. Tanaka, K. Shizu, H. Miyazaki and C. Adachi, *Chem. Commun.*, 2012, **48**, 11392-11394.
8. M. Kim, S. K. Jeon, S.-H. Hwang and J. Y. Lee, *Adv. Mater.*, 2015, **27**, 2515-2520.
9. D. R. Lee, M. Kim, S. K. Jeon, S.-H. Hwang, C. W. Lee and J. Y. Lee, *Adv. Mater.*, 2015, **27**, 5861-5867.
10. W.-L. Tsai, M.-H. Huang, W.-K. Lee, Y.-J. Hsu, K.-C. Pan, Y.-H. Huang, H.-C. Ting, M. Sarma, Y.-Y. Ho, H.-C. Hu, C.-C. Chen, M.-T. Lee, K.-T. Wong and C.-C. Wu, *Chem. Commun.*, 2015, **51**, 13662-13665.
11. T.-A. Lin, T. Chatterjee, W.-L. Tsai, W.-K. Lee, M.-J. Wu, M. Jiao, K.-C. Pan, C.-L. Yi, C.-L. Chung, K.-T. Wong and C.-C. Wu, *Adv. Mater.*, 2016, **28**, 6976-6983.